ACS Infectious Diseases

Article

pubs.acs.org/journal/aidcbc

Immunodominant SARS Coronavirus Epitopes in Humans Elicited both Enhancing and Neutralizing Effects on Infection in Non-human Primates

Qidi Wang,[‡,∥] Lianfeng Zhang,[§,∥] Kazuhiko Kuwahara,[Δ,∥] Li Li,[‡] Zijie Liu,[‡] Taisheng Li,[⊥] Hua Zhu,[§] Jiangning Liu,[§] Yanfeng Xu,[§] Jing Xie,[⊥] Hiroshi Morioka,[Δ] Nobuo Sakaguchi,[*,Δ,⊗] Chuan Qin,[*,§] and Gang Liu[*,†,‡]

[†]Tsinghua-Peking Center for Life Sciences & School of Pharmaceutical Sciences, Tsinghua University, Haidian District, Beijing 100084, People's Republic of China

[‡]Institute of Materia Medica, Chinese Academy of Medical Sciences & Peking Union Medical College, 2A Nanwei Road, Xuanwu District, Beijing 100050, People's Republic of China

[§]Institute of Laboratory Animal Science, Chinese Academy of Medical Sciences and Peking Union Medical College, Beijing 100021, People's Republic of China

[Δ]Faculty of Life Sciences, Kumamoto University, 1-1-1 Honjo, Kumamoto 860-8556, Japan

[⊥]Department of Infectious Disease, Peking Union Medical College Hospital and AIDS Research Center, Chinese Academy of Medical Sciences and Peking Union Medical College, Beijing 100071, People's Republic of China

[⊗]WPI Immunology Frontier Research Center, Osaka University, 3-1 Yamada-oka, Suita, Osaka 565-0871, Japan

Supporting Information

ABSTRACT: Severe acute respiratory syndrome (SARS) is caused by a coronavirus (SARS-CoV) and has the potential to threaten global public health and socioeconomic stability. Evidence of antibody-dependent enhancement (ADE) of SARS-CoV infection in vitro and in non-human primates clouds the prospects for a safe vaccine. Using antibodies from SARS patients, we identified and characterized SARS-CoV B-cell peptide epitopes with disparate functions. In rhesus macaques, the spike glycoprotein peptides $S_{471–503}$, $S_{604–625}$, and $S_{1164–1191}$ elicited antibodies that efficiently prevented infection in non-human primates. In contrast, peptide $S_{597–603}$ induced antibodies that enhanced infection both in vitro and in non-human primates by using an epitope sequence-dependent (ESD) mechanism. This peptide exhibited a high level of serological reactivity (64%), which resulted from the additive responses of two tandem epitopes ($S_{597–603}$ and $S_{604–625}$) and a long-term human B-cell memory response with antisera from convalescent SARS patients. Thus, peptide-based vaccines against SARS-CoV could be engineered to avoid ADE via elimination of the $S_{597–603}$ epitope. We provide herein an alternative strategy to prepare a safe and effective vaccine for ADE of viral infection by identifying and eliminating epitope sequence-dependent enhancement of viral infection.

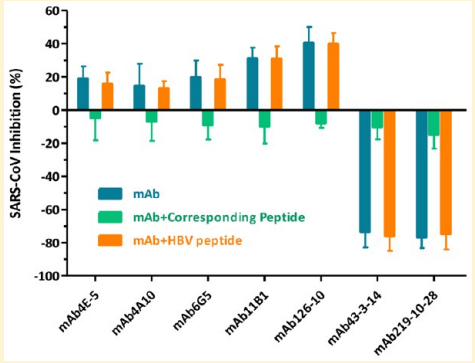

KEYWORDS: *SARS-CoV, peptide, vaccine, antibody-dependent enhancement (ADE), epitope sequence-dependent (ESD) enhancement, B-cell peptide epitope*

A novel severe acute respiratory syndrome coronavirus (SARS-CoV) was characterized in March 2003 after a global effort following the first epidemiological case in November 2002.[1] Ten years later (2012), a novel Middle East respiratory syndrome (MERS) coronavirus emerged, which was a β-coronavirus, similar to SARS-CoV.[2] SARS is a deadly infectious disease and has the potential to seriously threaten public health and socioeconomic stability worldwide.[1] Serologic and genetic investigations indicate that SARS-CoV is of zoonotic origin,[3,4] with bats as the likely animal reservoir. Since the identification of SARS-CoV in 2003, there have been major advances in understanding SARS-CoV genetics[1,5,6] and molecular epidemiology[7] and in identification of host receptors[8,9] and T-cell epitopes.[10,11] Models in mice, ferrets, and monkeys have been established, each with particular strengths and weaknesses.[12] Vaccine candidates have included DNA, a live attenuated strain, recombinant proteins, inactivated whole virions, and vector vaccines;[13] however, none have been approved through clinical investigation.[14] Safety concerns about a SARS-CoV vaccine have been raised, given the observation in vitro of antibody-dependent

Received: January 7, 2016
Published: March 30, 2016

DOI: 10.1021/acsinfecdis.6b00006
ACS Infect. Dis. 2016, 2, 361−376

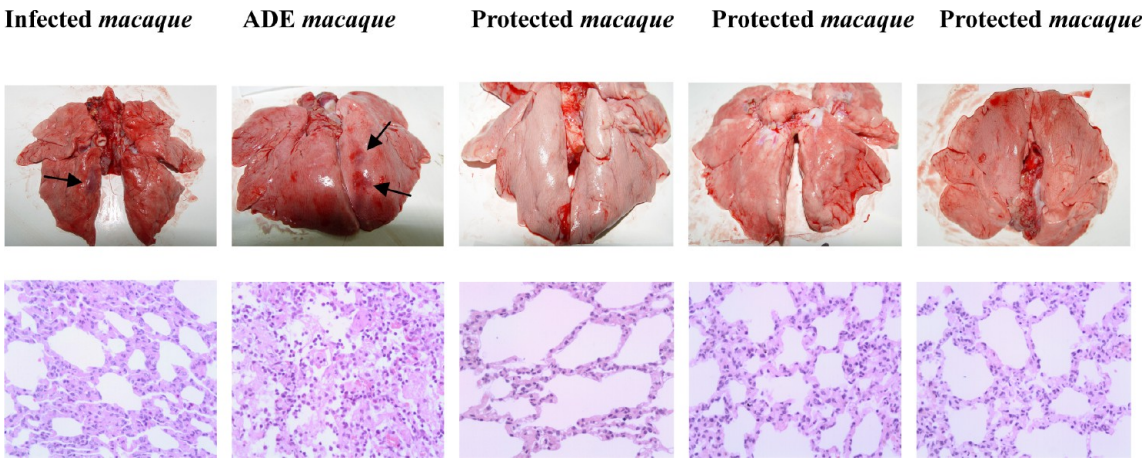

Figure 1. Observation of ADE induced by inactivated SARS-CoV vaccine in the lungs (H&E staining, 200×). The monkeys were immunized intramuscularly with formalin-inactivated SARS-CoV virions and boosted on day 14 with the same dose of 1.0 mL/monkey (4×10^4 $TCID_{50}$). The animals were then challenged with nasal cavity inoculation of SARS-CoV (1×10^6 $TCID_{50}$ in 4.0 mL/monkey, PUMC01 SARS-CoV strain) 14 days after the boost. The animals were sacrificed 6 days after viral challenge, and lung tissues were sampled for general and pathological observations. Pathological examination procedures were as described in ref 37. Infected macaque: lung interval broadened, visible macrophage infiltration with alveolar epithelial hyperplasia. ADE macaque: lung interval broadened, lung interval fractured with large amounts of macrophage and lymphocyte infiltration, visible fibrin and protein-rich edema in alveolar cavity. Protected macaques: lung interval slightly broadened, without visible abnormalities. The arrows indicate the lung lesions of infected and ADE animals.

enhancement (ADE) of SARS-CoV infection that could, in theory, exacerbate disease.[15] Other observations include evidence of ADE reported here for the first time induced by an inactivated SARS-CoV vaccine in rhesus macaques (Figure 1) and by antisera from SARS patients (Table S1), as well as ADE in other coronavirus infections.[16−18]

ADE in vitro has been observed for many other viruses, including yellow fever virus, West Nile virus, human immunodeficiency virus (HIV), Ebola virus, respiratory syncytial virus (RSV), and influenza A virus.[19−21] HIV-induced ADE has been described,[22,23] but the exact mechanism is still uncertain.[24] Among other examples of ADE, secondary infection with dengue virus of a heterologous serotype has been associated with an immunopathologic vascular leakage and hemorrhagic syndrome, Dengue hemorrhagic fever/dengue shock syndrome (DHF/DSS).[25] Most descriptions of ADE relate to Fc-gamma receptor (FcγR) and/or complement components promoting viral uptake and virus replication pathways.[26−28] Goncalvez et al. reported that treatment of juvenile rhesus monkeys with the cross-reactive mAb 1A5, which recognizes the fusion loop in DII of Dengue virus, enhanced DV4 viremia by several logs within 3−6 days of infection.[26] Furthermore, a 9-amino acid (aa) deletion at the N-terminus of the CH_2 domain in the Fc region abrogated enhancement in vitro and in vivo, confirming that ADE occurred through an FcγR pathway for this class of antibodies. Another study analyzed the stoichiometric relationship between antibody-mediated neutralization and enhancement of West Nile virus (WNV) infection in cells expressing FcγR.[29] The results showed that there is an antibody occupancy threshold on the virion for neutralization or enhancement of virus infection. Strongly neutralizing DIII-lateral ridge-specific mAbs inhibit at lower occupancy, whereas weakly neutralizing mAbs that bind distinct epitopes require a much higher mAb occupancy for neutralization. When mAb occupancy falls below the threshold for neutralization, ADE can occur. In subsequent studies, the same group showed that the level of antibody occupancy that promotes ADE in vivo is also modulated by the binding of C1q, which restricts ADE in an IgG subclass-specific manner.[30] On the basis of these studies, many neutralizing antibodies may enhance infection in vitro in $FcγR^+$ cells when their concentrations fall below a key occupancy threshold, and some Abs that poorly neutralize may strongly enhance over a wide dose−response range. However, for antibody isotypes that bind C1q avidly, much of the enhancing effect may be minimized in vivo.

Other studies suggest that FcγR-dependent ADE may not be the only mechanism for antibody enhancement of infection. Huang et al.[31] demonstrated ADE in vitro of an anti-prM mAb against DENV in cell lines that lacked expression of FcγR (e.g., baby hamster kidney cell line BHK-21 and murine fibroblast cell lineNIH3T3). Importantly, a peptide in the M3 region (CPFLKQNEPEDIDCW) of prM blocked this ADE in a dose-dependent manner. The antibody appeared to have dual specificity and bound to Dengue virus virions and/or a cross-reactive HSP60 protein on the cell surface. Thus, ADE via non-FcγR- or complement-dependent mechanisms is plausible for DENV, yet poorly characterized in vitro and in vivo. Herein, we discovered that a peptide of the viral sequence simultaneously elicits the antibodies of disparate functions in protection and enhancement against SARS-CoV infection by the studies with host Vero E6 cells in vitro and in non-human primates.

RESULTS

Observation of ADE Induced by Inactivated SARS-CoV Vaccine in the Lungs of Macaques. First, we observed the ADE of SARS-CoV infection in lungs after immunization with the inactivated virus vaccine in macaques. The monkeys with or without the immunization of inactivated SARS-CoV vaccine were infected by nasal cavity inoculation of live SARS-CoV virions (Figure 1). Infected macaques showed lungs with broadened interval and visible macrophage infiltration with alveolar epithelial hyperplasia. However, ADE macaques after vaccination showed lungs with broadened interval, lung interval fractured with large amounts of macrophage and lymphocyte infiltration, visible fibrin, and protein-rich edema in the alveolar cavity. Protected macaques showed lungs with slightly

DOI: 10.1021/acsinfecdis.6b00006
ACS Infect. Dis. 2016, 2, 361−376

Table 1. Peptides Recognized by SARS-Infected Patients, Relevant Mouse mAbs, and Functional Classification[a]

Peptide	Sequence*	Serologic reactivity#	mAb	Isotype (Fc)	Binding affinity to peptide (Molar)	Function$^{\zeta}$
$S_{471-503}$	H-ALNCYWPLNDYG FYTTTGIGYQPYRV VVLSFEL-NH_2	12.8%	4E5	IgG1/κ	4.67×10^{-9}	Neu
			4A10	IgG1/κ	2.96×10^{-9}	Neu
			6G5	IgG2b/κ	5.82×10^{-9}	Neu
$S_{604-625}$	H-TDVSTAIHADQL TPAWRIYSTGC-NH_2	32.6%	11B1	IgG2a/κ	2.32×10^{-9}	Neu
$S_{597-625}$	H-LYQDVNCTDVST AIHADQLTPAWRIY STG-NH_2	64.0%	43-3-14	IgG1/κ	1.21×10^{-11}	ADE
			219-10-28	IgG1/κ	1.20×10^{-8}	ADE
$S_{1164-1191}$	H-EIDRLNEVAKNL NESLIDLQELGKYE QYC-NH_2	13.9%	126-10	IgG1/κ	4.59×10^{-9}	Neu

[a]*, red-, blue-, and green-colored peptides represent the epitopes that were assembled into immunogenic peptides. ζ, neu (neutralizing) or ADE indicates the ability of the individual mAb to block or enhance, respectively, SARS-CoV infection of Vero E6 cells. #, the reactivity of individual peptides with antisera from 470 convalescent SARS patients (male, 192; female, 278) was determined using an ELISA. Commercially available ELISA kits were used to confirm that 81% of the 470 antisera were positive against viral lysates as antigen (cutoff value = 0.1). The titer of each serum was averaged from duplicate wells.

broadened intervals without visible abnormalities. The results implied that the simple vaccination with inactivated whole SARS-CoV virions might be ineffective for protection of virus infection.

Identification of Highly Immunodominant B-Cell Peptides of SARS-CoV in Humans. Mapping highly immunoreactive human B-cell peptides by employing SARS patient antisera was carried out by a number of research groups. Consistent with previous reports, Jiang's laboratory reported that the M1−131 and M132−162 peptides[32] from the membrane protein and the N153−178 and N362−412 peptides from the N protein[33] were highly reactive with all convalescent-phase test sera from SARS patients. The laboratories of Wu and Che collaboratively identified three conformational (amino acids 1−69, 68−213, and 337−422) and three linear (amino acids 1−69, 121−213, and 337−422) epitopes on the full-length N protein that were immunodominant.[34] Using a "split and mix" combinatorial strategy, we synthesized an overlapping peptide library spanning all four structural proteins of the SARS-CoV BJ01 strain, including the envelope (E), membrane (M), nucleocapsid (N), and spike (S). We screened this peptide library with antisera from convalescent SARS patients and identified dominant peptide epitopes recognized by anti-SARS IgG.[35] Further experiments in this paper indicate that three peptides in the S protein ($S_{471-503}$, $S_{604-625}$, and $S_{1164-1191}$) were strongly bound by SARS-CoV-specific human IgG from 12.8, 32.6, and 13.9%, respectively, of the 470 SARS patients (Table 1). Extension of the peptides (Table S2) to further characterize the epitopes' N- and C-termini identified a new immunodominant peptide ($S_{597-625}$), which was recognized by antisera from 64% of the patients (Table 1). The $S_{597-625}$ peptide specifically reduced the titer of human IgG in convalescent sera from SARS patients who reacted with SARS-CoV viral lysates (Figure 2A). We studied sequentially collected sera from 21 convalescent SARS patients whose sera (obtained 3 months after onset of infection) strongly reacted with the $S_{597-625}$ peptide. The antisera from these patients continued to recognize the $S_{597-625}$ at 12 months [12/21 (57.1%)], 18 months [7/21 (33.3%)], and 24 months [6/21 (28.6%)] after the onset of SARS (Figure 2B), implying that the $S_{597-625}$ peptide is a major immunodominant peptide in humans and elicits a long-term B-cell memory response after natural infection with SARS-CoV.

Epitope-Specific Antibodies of SARS-CoV Exhibited Enhancing or Neutralizing Functions in Vitro. To study the functional significance of immunodominant peptides of the S glycoprotein, we generated 23 monoclonal antibodies (mAbs, Table S3) by immunization of mice. Ten of these strongly bound to the SARS-CoV virion (Figure 3A). Among them, five blocked SARS-CoV infection of Vero E6 cells (Figure 3B), including mAb4E5, mAb4A10, and mAb6G5 against $S_{471-503}$, mAb11B1 against $S_{604-625}$, and mAb126−10 against $S_{1164-1191}$.

In contrast, two mAbs (mAb43-3-14 and mAb219-10-28) against $S_{597-625}$, despite sharing some of the same isotypes and constant region configurations with neutralizing antipeptide antibodies (IgG1/κ, IgG2a/κ, and IgG2b/κ; Table 1), markedly enhanced SARS-CoV infection of Vero E6 cells (Figure 3B). This was particularly striking given that Vero E6 cells lack FcγR, and the best-understood mechanism for ADE involves Fc-mediated internalization and replication of virus. mAb43-3-14-

DOI: 10.1021/acsinfecdis.6b00006
ACS Infect. Dis. 2016, 2, 361−376

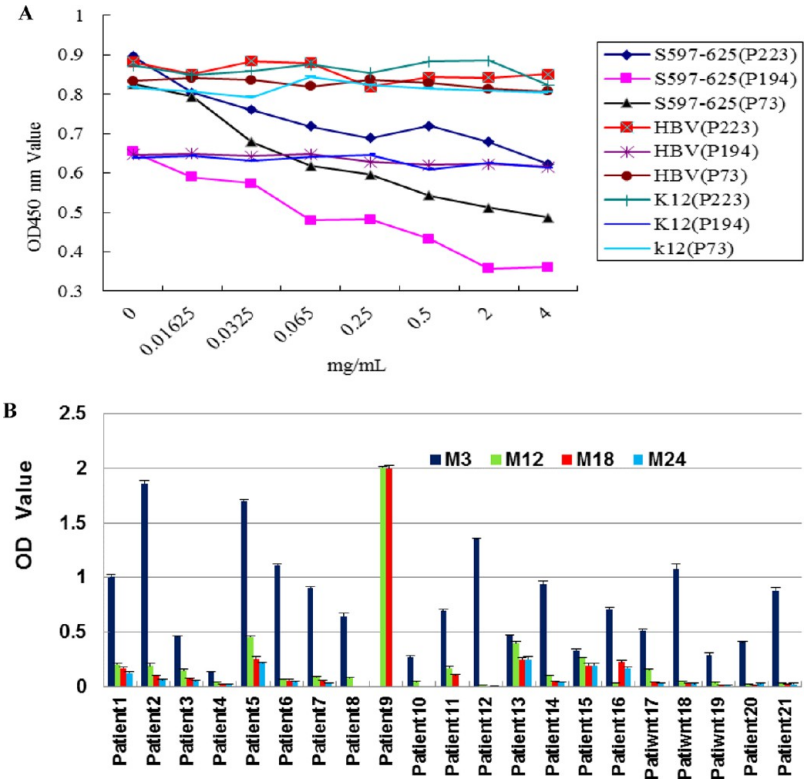

Figure 2. Immunogenic specificity and long-term memory response of IgG from antisera of SARS patients to $S_{597-625}$ peptide. (A) The reactivity of human IgG to SARS viral lysates (ELISA kit: Huada S20030004, Beijing, China) is specifically reduced in a dose-dependent manner by $S_{597-625}$, but not by the hepatitis B virus (HBV) peptide MDIDPYKEFGATVELLSFLP. P223, P73, and P194 represent three antisera from convalescent SARS patients. Reactivity of human IgG with the $S_{597-625}$ peptide was determined by an ELISA. Lysates (0.025 μg/well) were incubated overnight at room temperature and then blocked by 5% goat serum in PBS (125 μL) for 2 h. Ten microliters of antiserum and 100 μL of PBS were further incubated for 30 min at 37 °C. Proper amounts of goat anti-human IgG conjugated to HRP were used for detection of OD_{450} values. Each antiserum was used in duplicate, and the cutoff value was 0.1. (B) The antisera of 21 convalescent SARS patients were collected and tested 3 (M3), 12 (M12), 18 (M18), and 24 (M24) months after onset of SARS-CoV infection. The antiserum of patient 9 collected 3 months after onset of infection was omitted due to insufficient sample quantity. The peptides were dissolved in a minimal volume of DMSO and then diluted to a final concentration of 10 μg/mL in carbonate buffer (pH 9.6). In total, 1.0 μg/well was used for capture antibodies from antiserum. The detailed procedure was the same as in (A) with a cutoff value of 0.1.

and mAb219-10-28-enhanced Vero E6 cell infection was reduced in a dose-dependent manner by $S_{597-625}$, but not by an unrelated HBV peptide (Figure 4A,B), whereas ADE of human antisera from SARS-CoV-infected patients was also specifically blocked by the same peptide (Figure 4C,D), implying that peptide-based ADE occurred during the epidemic period of a SARS outbreak.

An antibody-peptide binding ELISA indicated that mAb11B1 against $S_{604-625}$ reacts with both $S_{597-625}$ and $S_{604-625}$, whereas mAb43-3-14 against $S_{597-625}$ only bound to $S_{597-625}$ (Figure 4E). The data suggest that mAb11B1 was induced by $S_{604-625}$ and is a consensus peptide of $S_{597-625}$ and $S_{604-625}$, whereas mAb43-3-14 was from the N-terminal peptide $S_{597-603}$ (LYQDVNC) immunizing antigen. Synthesized peptides LYQDVN ($S_{597-602}$), LYQDVNC ($S_{597-603}$), and LYQDVNCT ($S_{597-604}$) were all immunoreactive with the tested sera of 24 SARS-positive patients, further confirming that the $S_{597-603}$ peptide is an immunodominant one in humans (Figure S1). Alanine scanning mutagenesis of the $S_{597-604}$ peptide demonstrated that L597, Y598, Q599, D600, and C603 are critical amino acid residues for interaction with mAb43-3-14 (Figure 4E; Table S4). The $S_{597-603}$ peptide lies close to the C-terminus of the SARS-CoV major receptor (ACE2)-binding domain (RBD).[8] We speculate that mAb43-3-14 may expose specific conformations that catalyze SARS-CoV attachment to and/or membrane fusion with target cells.

Neutralization or Enhancement of SARS-CoV Infection in Non-human Primates by Epitope-Specific Antibodies. Low-molecular-weight peptides behave like haptens, with relatively low immunogenicity. To make them more immunogenic, we chemically ligated four copies of each peptide to a lysine core [$BrCH_2CO$-Lys_2-(Lys)-β-Ala-$CONH_2$(BrK_2KA), Scheme 1] to prepare a multiple antigen peptide system (MAP)[36] and purified them by preparative HPLC (Figure 5A; Table S7). Molecular weight was confirmed by LC-MS/MS (Figure 5B).

We used these synthetic MAPs to vaccinate rhesus monkeys (Table S4) as follows: Vac1, control group (received 0.9% NaCl) of four macaques randomly assigned to two groups for day 2 or day 6 postinfection sacrifice; Vac2, MAP-$S_{597-625}$ given to six macaques randomly assigned to two groups for day 2 or day 6 postinfection sacrifice; Vac3, a mixture of MAP-$S_{471-503}$, MAP-$S_{604-625}$, and MAP-$S_{1164-1191}$ given to six macaques randomly assigned to two groups for day 2 or day 6 postinfection sacrifice; and Vac4, a mixture of MAP-$S_{471-503}$, MAP-$S_{597-625}$, and MAP-$S_{1164-1191}$ given to six macaques randomly assigned to two groups for day 2 or day 6 postinfection sacrifice. The immunization protocol included one priming injection followed by three boosts at 2-week intervals (Chart S1). Antipeptide polyclonal Abs (monkey IgG) monitored by ELISA showed high-level responses to all immunized peptides after three boosts (Figure 6, left).

DOI: 10.1021/acsinfecdis.6b00006
ACS Infect. Dis. 2016, 2, 361−376

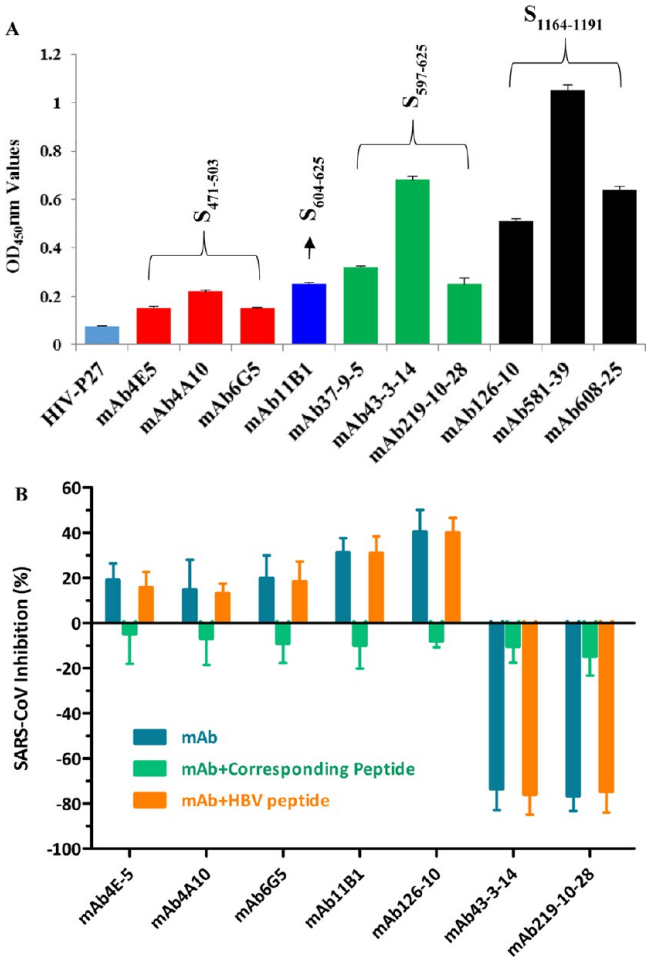

Figure 3. Generated monoclonal antibodies bound to SARS-CoV virions and shared disparate functions. (A) The defined monoclonal antibodies bound to SARS-CoV virions of SARS-CoV PUMC01 strain (4×10^{-5} $TCID_{50}$/mL).[46] The cutoff value was set to 0.1 (the average for binding of unrelated mAb-HIV-P27). (B) Neutralization or enhancement of the SARS-CoV infection in Vero E6 cells by mAbs (1.0 μg/mL) was specifically reduced by the corresponding immunopeptide (0.1 μg/mL), but not by a hepatitis B virus (HBV) peptide (0.1 μg/mL). HBV peptide (LLDYQGMLPV) is an unrelated control peptide from an HBV surface protein. $S_{597-625}$ and HBV peptide were pre-incubated with the corresponding mAbs or human antisera for 30 min at 4 °C before function was tested. These experiments were performed in triplicate, and the data are presented as the mean ± standard deviation.

Antibodies (Figure 6A) against the four peptides in sera from Vac1-immunized animals were at background level on all blood collection days. Vac2 gradually induced anti-$S_{597-625}$ peptide antibodies after three boosts. Not surprisingly, both Vac2 and Vac4 immunizations elicited high levels of IgG against the $S_{604-625}$ peptide because the vaccine components consisted of the $S_{597-625}$ or $S_{604-625}$ epitopes in these two animal groups. Anti-$S_{604-625}$ and -$S_{1164-1191}$ antibodies in the Vac3-immunized animal group reached their highest levels before the second boost (28 days after the first injection). The average titer of anti-$S_{604-625}$ IgG was greater than $1:10^6$ in Vac3-immunized monkeys before SARS-CoV challenge and was 3- or 2-fold times that of Vac2 or Vac4, respectively. Interestingly, when Vac3-vaccinated animals were challenged by SARS-CoV, the IgG level against $S_{604-625}$ gradually decreased (Figure 6B) on days 2 and 6 postinfection. This is different from the Vac2 and Vac4 immunizations, after which IgG levels inexplicably increased on day 2 postinfection and subsequently decreased on day 6 postinfection. This observation implies that anti-$S_{604-625}$ antibodies are strongly involved in the neutralization of SARS-CoV in monkeys and that the existing $S_{597-603}$ epitope (in Vac2 and Vac4) may reduce the total titer of anti-$S_{604-625}$ antibodies.

All immunized macaques were subsequently challenged with SARS-CoV (PUMC01 strain) via nasal inhalation on the 14th day after the last boost, as described.[37] At 2 and 6 days postinfection (DPI), the macaques were sacrificed (Chart S1; Table S7). The data for lung damage and viral burden in these macaques are summarized in Table 2.

Gross lung pathology was evident at both 2 and 6 DPI in all groups. In mock-immunized macaques (Vac1), the average pathology grade was grade IV (Figure 7A,B; Table S5), with severe diffuse alveolar damage, including alveolar shrinking and rupture of elastic fibers. Massive macrophage infiltration was associated with fusion of alveolar septa. Pulmonary edema, fibrin, hemorrhage, and cellular debris contributed to the severe interstitial pneumonitis. Damage was similar (grade IV) for Vac2, somewhat reduced (grade II−III) for Vac4, and markedly diminished (grade I−II) for Vac3. Immunohistochemistry using mAbs against the viral peptides revealed a large number of SARS-CoV-infected macrophages and alveolar epithelial cells in the Vac1 group (Figure 7C), averaging 13.5 ± 2.6 infected cells per 10 high-power fields (HPF) and 10.0 ± 3.0 infected cells per 10 HPF at 2 and 6 DPI, respectively. Quantitative viral burden analysis by quantitative RT-PCR showed an average of 141,000 copies/mg lung tissue (2 DPI) and 136,000 copies/mg lung tissue (6 DPI) of SARS-CoV in the lungs of the Vac1 group.

Compared with the Vac1 group, the Vac2 group showed similar histology at 2 DPI, but the interstitial pneumonia was far worse at 6 DPI, characterized by massive numbers of inflammatory cells in hemorrhagic septa, with extensive exudation. SARS-CoV-infected cells in the lungs averaged 13.8 ± 2.1 per 10 HPF at 2 DPI and 9.8 ± 3.0 per 10 HPF at 6 DPI, whereas viral copies were 116,000/mg lung tissue and 143,000/mg lung tissue, respectively. Thus, even though $S_{597-625}$ was immunodominant in patients, antigenic in monkeys, and reactive with the neutralizing mAb 11B1, it was nonprotective and even harmful when used as a vaccine.

In contrast, the immunized monkeys in the Vac3 group had a strongly increased ability to control SARS-CoV infection in association with induction of high levels of anti-$S_{604-625}$ antibodies (Figure 7E). At 2 DPI, hemorrhage in septa and elastic fibers of the alveolar wall were indicated by apparent inflammation in silver staining results. Alveolus septa broadening with increasing infiltration of inflammatory cells were recorded by 6 DPI, indicating that only early, acute diffuse alveolar damage occurred. SARS-CoV-infected lung cells in the Vac3 group averaged 7.4 ± 3.2 per 10 HPF (vs Vac1 group: $p < 0.01$) and 7.0 ± 2.9 per 10 HPF (vs Vac1 group: $p < 0.01$) at 2 and 6 DPI, respectively. The SARS-CoV burden averaged 6,200 copies/mg lung tissue at 2 DPI and 7,300 copies/mg lung tissue at 6 DPI. This represents a ratio of ~19 and ~20 between the number of SARS-CoV copies in the Vac3 and Vac1 groups at 2 and 6 DPI, respectively.

For animals that received Vac4, symptoms of acute diffuse alveolar damage were visible, including fusion of thick septa and ruptured elastic fibers of the alveoli. The average number of SARS-CoV infected cells in the lung tissues was 8.14 ± 3.32 per 10 HPF at 2 DPI (vs Vac1 group: $p < 0.01$) and 7.8 ± 2.91 per 10 HPF at 6 DPI (vs Vac1 group: $p < 0.01$). The SARS-CoV burden

DOI: 10.1021/acsinfecdis.6b00006
ACS Infect. Dis. 2016, 2, 361−376

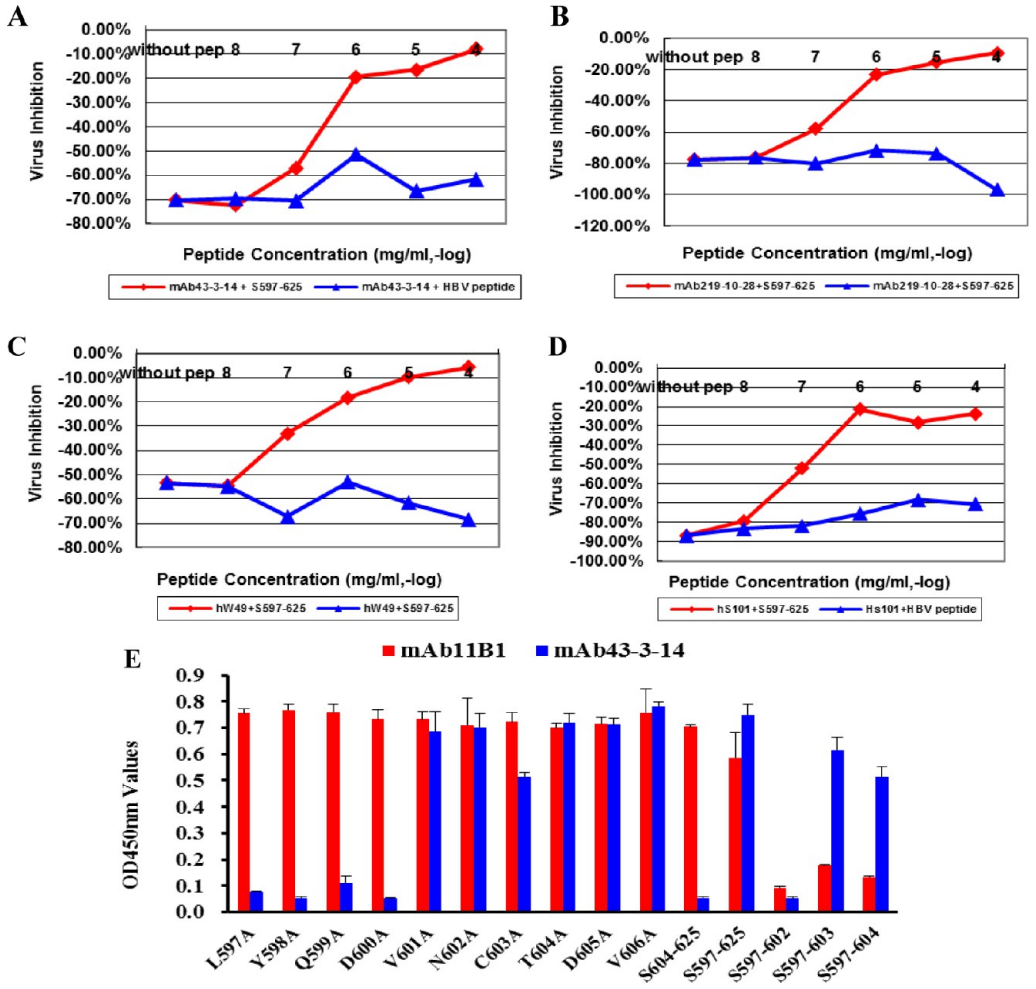

Figure 4. Antibody-dependent enhancement of SARS-CoV infection. (A–D) Enhancement of SARS-CoV infection by either mAbs (1.0 μg/mL) or human antisera (1:500) was reduced in a peptide dose-dependent manner. hW49 and hS101 represent two antisera from convalescent SARS patients 3 months after onset. HBV peptide (LLDYQGMLPV) is an unrelated control peptide from HBV surface protein. $S_{597-625}$ and HBV peptide were pre-incubated with the corresponding mAb or human antisera for 30 min at 4 °C before function was tested. (E) Alanine scanning mutagenesis of the $S_{597-606}$ showed the minimum requirement ($S_{597-603}$) for N-terminal binding of $S_{597-625}$ to mAb43-3-14. This experiment was performed in triplicate, and the data are presented as the mean ± standard deviation.

averaged 31,254 copies/mg lung tissue at 6 DPI, that is, 4.5 times the burden of 6,835 copies/mg lung tissue at 2 DPI. The Vac4 group also showed a 4.3-fold increase to Vac3 group (31,254 copies/mg vs 7,300 copies/mg) of viral burden at 6 DPI, suggesting that the presence of IgG against $S_{597-603}$ facilitated SARS-CoV infection of immunized macaques.

In a separate experiment focused on the phenomenon of ADE in macaques, rhesus monkeys were divided into six groups ($n = 3$ per group, Table S9). Three groups were separately sacrificed at 2 or 6 DPI; each time point included a control group and two groups that received the enhancing mAb43-3-14 at doses of 0.2 mg/kg or 1.8 mg/kg 1 day prior to challenge with the SARS-CoV PUMC01 strain. Gross pathologic changes were again recorded in the control group at a grade IV level (Figure 8A,B). Although clear pathologic changes were observed in one of the three monkeys in the 0.2 mg/kg group, we concluded that previous treatment with a dose of 0.2 mg/kg mAb43-3-14 did not, on average, significantly reduce or facilitate SARS-CoV infection. However, macaques treated with 1.8 mg/kg mAb43-3-14 showed a marked increase in lung lesions. The lung lesion area in macaque D4-060060 (4.0 × 2.5 cm^2) at 6 DPI was the largest in all dic experimental groups. At 6 DPI, all lungs from the 1.8 mg/kg group showed larger areas of necrosis, severe sheets of septa fusion, necrotic lesions at the hemorrhagic septa, and massive macrophage infiltration in the alveoli, indicating that the interstitial pneumonia was much more severe in the mAb43-3-14-treated group than in the control group (Figure 8C). There were more SARS-CoV-infected cells in the lung tissue (12.5 ± 2.3 per 10 HPF at 2 DPI and 13.4 ± 2.6 per 10 HPF at 6 DPI, $p < 0.01$ vs control group). The average SARS-CoV burden in the lungs was 911,000 copies/mg lung tissue at 2 DPI and 944,000 copies/mg lung tissue at 6 DPI, a 10-fold enhancement compared with the control group at 2 DPI and a 14-fold enhancement at 6 DPI (Figure 8D). This result further confirmed that enhancement of the SARS-CoV infection in macaques was directly related to antibodies against $S_{597-603}$.

DISCUSSION

In this study, we reported for the first time that a SARS-CoV inactivated vaccine could induce ADE and lung pathology in experimental rhesus monkeys. Four antigenic peptides ($S_{471-503}$, $S_{604-625}$, $S_{597-625}$, and $S_{1164-1191}$) from the spike protein of SARS-CoV were identified by high cross-reactivity with a large number of antisera from convalescent SARS patients. Ten of 23 mAbs

DOI: 10.1021/acsinfecdis.6b00006
ACS Infect. Dis. 2016, 2, 361–376

Scheme 1. Synthesis of Multiple Antigen Peptide Systems (MAPS) by Chemical Ligation of a Thiol Nucleophilic Substitution Reaction[a]

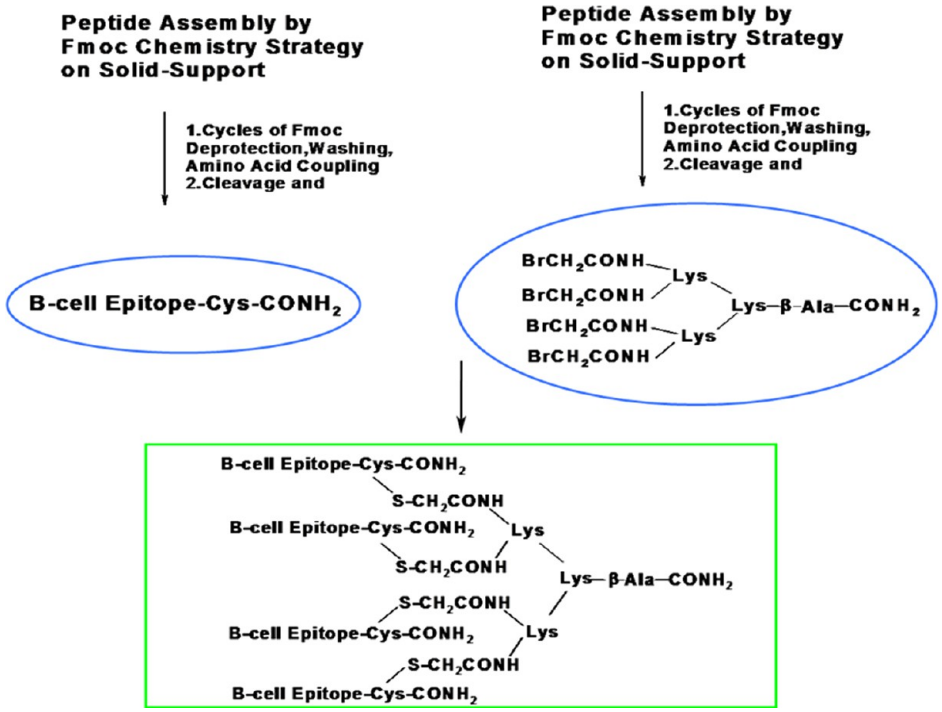

[a]B-cell epitopes with a free −SH sequence (containing a Cys residue) were prepared directly. B-cell epitopes without a free −SH group were anchored by an additional cysteine residue at the C-terminal (Figure S2). A four-branched, brominated, multiple-antigen core peptide (BrK_2KA, Figure S3) via lysine two α-amino and side-chain amino groups was prepared that finally conjugated with four copies of individual antigenic peptide.

generated against these four peptides bound to the SARS-CoV virion (Figure 3A), indicating that each peptide is exposed on the SARS-CoV surface. Among them, five mAbs against $S_{471-503}$, $S_{604-625}$, and $S_{1164-1191}$ blocked SARS-CoV infection of Vero E6 cells (Figure 3B), and two mAbs (mAb43-3-14 and mAb219-10-28) markedly enhanced SARS-CoV infection of Vero E6 cells. mAb43-3-14 alone significantly enhanced SARS-CoV infection at the tested high dose of 1.8 mg/kg in experimental rhesus monkeys, whereas Vac3 (consisting of $S_{471-503}$, $S_{604-625}$, and $S_{1164-1191}$ MAPs) successfully protected animals from SARS-CoV challenge and lung pathology. Alanine scanning mutagenesis indicated that L597, Y598, Q599, D600, and/or C603 are critical amino acid residues and that $S_{597-603}$ is responsible for mAb43-3-14-induced enhancement, which may catalyze SARS-CoV attachment and/or membrane fusion with target cells by exposing specific conformations of the spike protein.

$S_{471-503}$ is located at the virus RBD[8] and can block SARS-CoV infection of Vero E6 cells in vitro,[35] probably by interfering with high-affinity attachment of SARS virions to the human ACE2 receptor at residues T487 and N497 of the RBD.[38,39] The coronavirus spike proteins have been characterized as class I fusion proteins containing highly conserved heptad repeat regions (HR1 and HR2).[40] Thus, interfering with HR1 binding to HR2 has become a recent target for prevention of viral fusion and entry into target cells. $S_{1164-1191}$ overlaps HR2 (1145−1184 aa) in the SARS-CoV spike glycoprotein. The mechanism by which anti-$S_{1164-1191}$ antibodies reduce the efficiency of SARS-CoV fusion is likely to be associated with an exposed five-turn α-helix conformation via HR2 binding to HR1 and an extended conformation formed by residues 1160−1177 and 1178−1184 of three antiparallel HR2 helices in an oblique orientation surrounding a parallel, trimeric coiled-coil of three HR1 helices.[41]

Binding of mAb581-39 to the SARS-CoV virion was the strongest among the mAbs (Figure 3A), which implies that $S_{1164-1191}$ peptide may act as a major immunoantigen.

Severe lung injury occurred in one challenged rhesus monkey that had been immunized with an inactivated SARS-CoV vaccine (Figure 1). Very strong serologic reactivity of $S_{597-625}$ with antisera from 64.4% of convalescent SARS patients was observed; the response was to two tandem epitopes ($S_{597-603}$ and $S_{604-625}$), but each epitope generated antibodies with disparate functions regarding neutralization or enhancement of SARS-CoV infection. Thus, in persons infected by SARS-CoV, enhancing antibodies and neutralizing antibodies may partly counteract each other's functions.

SARS-CoV's ADE was also reported by other research laboratories. Using an HL-CZ human promonocyte cell line, Chen and Huang found that higher concentrations of antisera collected from SARS-CoV-infected patients facilitated SARS-CoV infection and induced higher levels of virus-induced apoptosis. They further demonstrated that this phenomenon occurred via antispike protein antibodies that mediated ADE, but not via anti-N protein antibodies.[42] Bruzzone and Jaume's laboratory showed that antispike immune serum increased infection of human monocyte-derived macrophages by replication-competent SARS-CoV as well as by spike-pseudotyped lentiviral particles (SARS-CoVpp), although they did not clarify whether this enhancement was through the FcγRII pathway.[43] Jaume et al. reported that a recombinant, full-length spike protein trimer potentiated infection of human B cell lines, despite eliciting a neutralizing and protective immune response in rodents. The study demonstrated that antispike immune serum, while inhibiting viral entry in a permissive cell line, potentiated infection of immune cells by SARS-CoV spike-pseudotyped

DOI: 10.1021/acsinfecdis.6b00006
ACS Infect. Dis. 2016, 2, 361−376

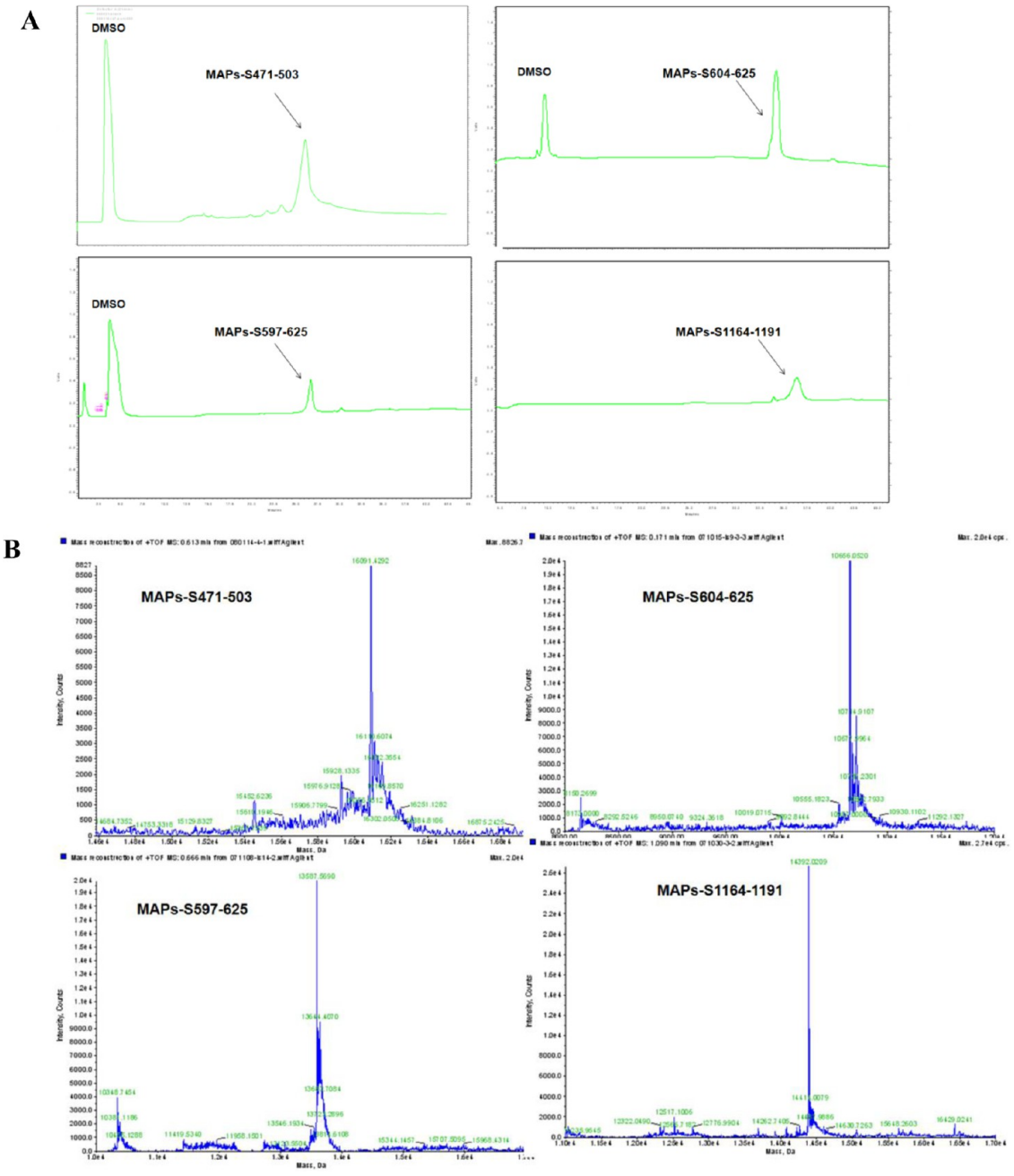

Figure 5. Tetrameric forms of peptides were successfully synthesized on a branched lysine scaffold. MAP-$S_{471-503}$ = $[(S_{471-503})_4Lys]_2Lys$-$\beta$-Ala-$CONH_2$; MAP-$S_{604-625}$ = $[(S_{604-625})_4Lys]_2Lys$-$\beta$-Ala-$CONH_2$; MAP-$S_{597-625}$ = $[(S_{597-625})_4Lys]_2$ Lys-β-Ala-$CONH_2$; MAP-$S_{1164-1191}$ = $[(S_{1164-1191})_4Lys]_2Lys$-$\beta$-Ala-$CONH_2$. RP-HPLC profiles (A) of the MAPs were analyzed by a Shimadzu LC-10AT analytical HPLC system with a C8 column (4.6 mm × 250 mm, 5 μm) and UV detection at 214 nm. The molecular weights (B) were determined by high-resolution LC-MS in an Agilent LC/MSD TOF system and hypermass reconstruction of the raw MS data to a single charge.

lentiviral particles, as well as by replication-competent SARS coronavirus. Jaume and collaborators proposed that ADE of SARS-CoV utilizes a novel cell entry mechanism into immune cells.[44]

This study demonstrates for the first time that an antibody (mAb43-3-14) targeting a specific linear epitope ($S_{597-603}$) of the SARS-CoV spike protein can mediate enhancement of virus infection both in vitro and in non-human primates via an epitope sequence-dependent mechanism. We also demonstrate that the viral peptides that induce protection from pathogenesis can be identified and distinguished from those inducing enhancement in primates. These findings reveal a new mechanism of virus evasion of host defense that potentially provides an alternative strategy to prepare safe and effective vaccines against ADE of virus infections.

MATERIALS AND METHODS

Peptide Design and Synthesis. New peptides from the spike glycoprotein were designed on the basis of the information gained in the first round of immunopeptide discovery.[32]

Peptides were synthesized manually by standard Fmoc chemistry protocols on Rink-amide MBHA resin (NovaBiochem, San Diego, CA, USA; 0.44 mmol/g). All of the L-α-Fmoc-protected amino acids and coupling reagents (DIC and HOBt)

DOI: 10.1021/acsinfecdis.6b00006
ACS Infect. Dis. 2016, 2, 361−376

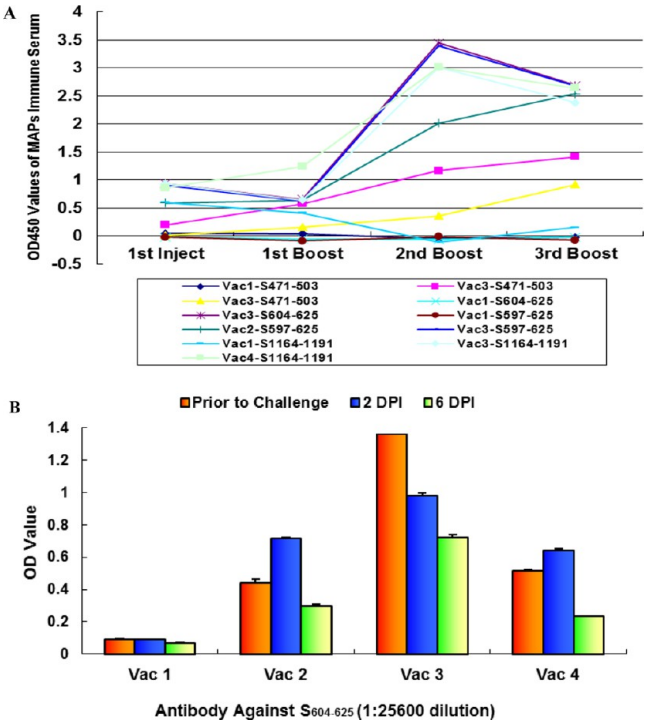

Figure 6. Rhesus monkeys strongly responded to peptide-based vaccines (Table S5). Vaccinations (A) were designed as Vac1 (0.9% NaCl) for the control group of four animals, Vac2 (MAPs-$S_{597-625}$) for the enhancement of SARS-CoV infection in six experimental animals, Vac3 (MAPs-$S_{471-503}$, MAPs-$S_{604-625}$, and MAPs-$S_{1164-1191}$) for the neutralization of SARS-CoV infection in six experimental animals, and Vac4 (MAPs-$S_{471-503}$, MAPs-$S_{597-625}$, and MAPs-$S_{1164-1191}$) for the reduction of neutralizing ability in six experimental animals (Table S4). The average IgG levels against peptides in each vaccine group were monitored by ELISA on the day before injection or boost. IgG level (B) against $S_{604-625}$ is an average of grouped macaques. The titer of anti-$S_{604-625}$ IgG was greater than $1:10^6$ in all relevant immunized monkey groups.

were obtained from GL Biochem (Shanghai, China). All solvents were of analytical grade and used without further purification. Each amino acid assembly was completed by using 3 equiv of L-α-Fmoc-protected amino acids and coupling reagents, and the ninhydrin colorimetric test after each coupling was carried out to ensure no detectable amino remaining. In the case that the peptide-bearing beads were colorized (positive) by ninhydrin test, the free amino group was then blocked by reacting with 15% acetic anhydride in dichloromethane (DCM) (v/v) for 30 min. Crude peptides without Cys, Met, Arg, and Trp residues were cleaved using a one-step TFA cleavage method under the following conditions: TFA (1.9 mL), deionized water (50 μL), and triethyl silane (50 μL). For peptides containing Cys, Met, Arg, or Trp residues, the following conditions were used: TFA (1.63 mL), thioanisole (0.1 mL), phenol (0.1 g), deionized water (0.1 mL), EDT (50 μL), and triethylsilane (20 μL). TFA solution was treated with ice-cooled diethyl ether to precipitate the peptide. The crude peptide was washed twice by ice-cooled diethyl ether and dried in the N_2 flow condition.

In particular, peptide $S_{471-503}$ was synthesized on SynPhase PA RAM D-series lanterns (loading 8 μmol/lantern, Mimotopes, Raleigh, NC, USA). The lanterns were treated with 20% piperidine in dimethylformamide (DMF) for 15 min for deprotection. The general coupling conditions for lanterns utilized a solution of 80% DMF and 20% DCM, with reagents at the following concentrations: AA, 120 mM; HOBt, 144 mM; DIC, 120 mM. For each lantern a minimum of 500 μL of the activated amino acid solution was required. Alternatively, bromophenol blue (5 μL/mL coupling solution, 5M) was used as an indicator to monitor the reaction. Simultaneous side-chain deprotection and cleavage were carried out using 2.5 mL per lantern of a solution of 82.5% trifluoroacetic acid (TFA)/5% thioanisole/5% anisole/5% water/2.5% 1,2-ethanedithiol for 2 h.

All crude peptides were purified by HPLC to >95% purity on a semipreparative RP C18 column (Zorbax, 300SB-C18, 9.4 × 250 mm. Agilent, Colorado Springs, CO, USA) eluting at 4 mL/min with a 0−20% CH_3CN (buffer B) gradient in water (buffer A) containing 0.1% TFA over 5 min followed by a 20−65% CH_3CN over 30 min. Pure peptides were identified by an Shimadzu LC-10AT analytic HPLC system with a C8 column (4.6 mm × 250 mm, 5 μm) and Agilent LC-MSD TOF (Figure S4; $S_{604-625}$, calculated 2505.83 Da, observed 2505.19 Da; $S_{1164-1191}$, calculated 3439.87 Da, observed 3438.70 Da; $S_{597-625}$, calculated 3238.62 Da, observed 3238.54 Da; $S_{471-503}$, calculated 3863.45 Da, observed 3864.20 Da). The molecular weight of peptides was calculated by a Peptide Molecular Weight Calculator of Biopeptide Co., Inc. (https://www.biopeptide.com/PepCalc/).

Synthesis and Characterization of Multiple Antigen Peptides (MAPs).[36] The branched lysine core ($BrCH_2CO$-Lys_2-(Lys)-β-Ala-$CONH_2$) scaffold was synthesized manually by standard Fmoc chemistry protocols on 0.22 mmol (500 mg) of Rink-amide MBHA resin (NovaBiochem, 0.44 mmol/g) as described above. *N*-α-Fmoc-Lys (Fmoc) was used at the branch points. The Fmoc-protected amino acids (5.0 equiv) were assembled by using 5.0 equiv of DIC coupling reagent and HOBt additive. The N-termini of the four branches of the lysine core were bromoacetylated on the resin with 10 equiv of bromoacetic acid and DIC in DMF for 2 h. The bromoacetylated lysine core was cleaved from the resin after treatment with 5% H_2O/95% TFA for 2 h. It was then precipitated with cold diethyl ether, lyophilized, and purified by HPLC on a semipreparative RP C18 column (Zorbax, 300SB-C18, 9.4 × 250 mm) eluting at 4 mL/

Table 2. Summary of Lung Damage and Viral Burden of Vaccinated Macaques Challenged by SARS-CoV

	gross lung pathology[a]		infected cells in lung[b]		viral burden[c]	
Vac	day 2	day 6	day 2	day 6	day 2	day 6
1	grade IV	grade IV	13.5 ± 2.6	10.0 ± 3.0	141,000	136,000
2	grade IV	grade IV	13.8 ± 2.1	9.8 ± 3.0	116,000	143,000
3	grade I−II	grade I−II	7.4 ± 3.2	7.0 ± 2.9	6,200	7,300
4	grade II−III	grade II−III	8.14 ± 3.32	7.8 ± 2.91	6,835	31,254

[a]Average gross lung pathology was determined by a standard in Table S8. [b]SARS-CoV-infected macrophages and alveolar epithelial cells in the vaccine groups were counted by using antipeptide antibodies. [c]Quantitative viral burden analysis by quantitative RT-PCR (viral copies/mg lung tissue).

DOI: 10.1021/acsinfecdis.6b00006
ACS Infect. Dis. 2016, 2, 361−376

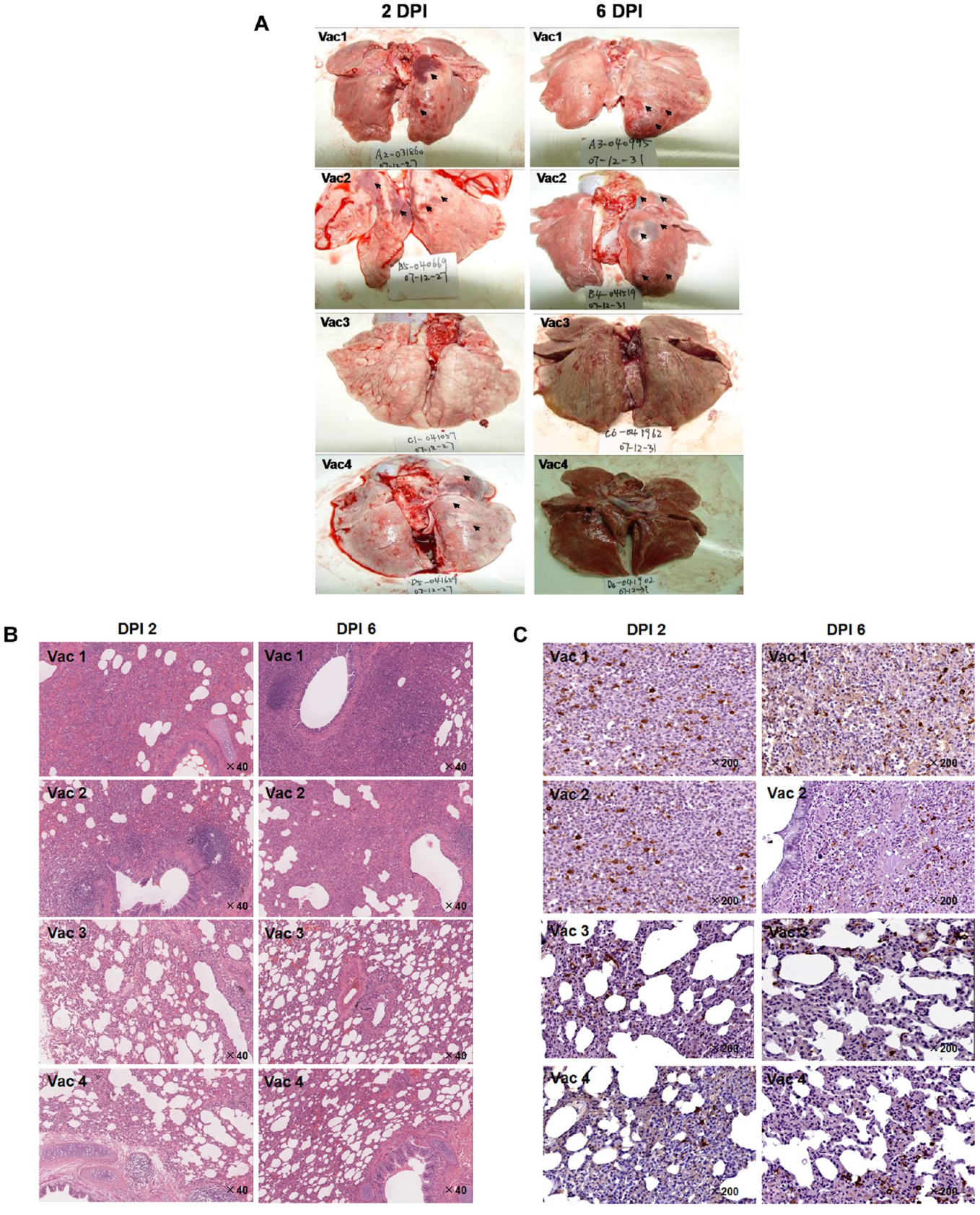

Figure 7. Peptide-based vaccines neutralized or enhanced SARS-CoV infection of rhesus monkeys. (A) Pathologic changes in lung tissue. The arrows point to the areas that showed pathology. (B) Histopathologic examination of macaque lung tissue. Lung damage was pathologically characterized as an average standard grade (Table S5). (C) Immunohistochemical staining of SARS-CoV-infected cells in lung tissue. Lung tissue sections were incubated with a mixture of mAb4E5, mAb11B1, and mAb9A6 (each at 0.01 μg/mL) and developed using horseradish peroxidase (HRP)-labeled goat anti-mouse IgG (1:1000 dilution, ZhongShan Inc., Guangzhou, PRC). SARS-CoV-positive cells show brown staining, which localizes in the cytoplasm of monocytes and pneumocytes (magnification 200×). Arrows indicate the lung lesions of animals.

DOI: 10.1021/acsinfecdis.6b00006
ACS Infect. Dis. 2016, 2, 361−376

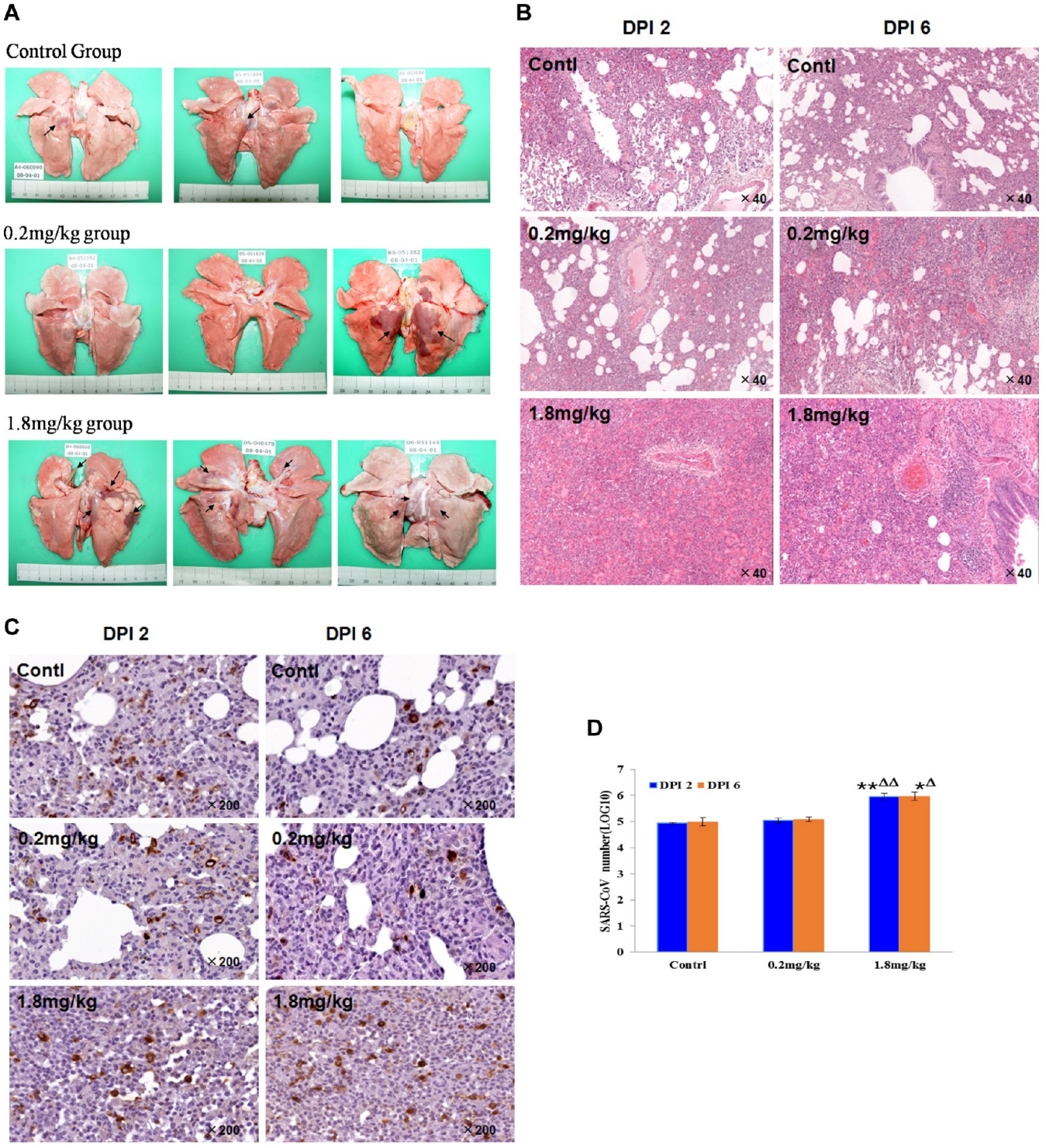

Figure 8. mAb43-3-14 enhances SARS-CoV infection of rhesus monkeys. (A) Pathologic changes at 6 DPI. (B) Histopathologic examination of macaque lung tissues. Lung damage was pathologically characterized as an average standard grade. Control group, grade IV; 0.2 mg/kg group, grade III–IV; 1.8 mg/kg group, grade IV. (C) Immunohistochemical staining of SARS-CoV-infected cells in lung tissue. The staining conditions were the same as in Figure 6. (D) SARS-CoV mRNA in infected monkey lung tissue was quantitatively analyzed from an average of three animals. The data are presented as the geometric mean ± standard deviation: (∗) $p < 0.05$; (∗∗) $p < 0.01$ versus control group; (Δ) $p < 0.05$; (ΔΔ) $p < 0.01$ versus 0.2 mg/kg group. Arrows indicate the lung lesions of animals.

min with a 0–20% CH_3CN gradient in water containing 0.1% TFA over 5 min followed by 20–40% CH_3CN over 20 min. Pure lysine core (25% yield) was identified by Agilent LC-MSD TOF: calculated (MH^+) 957.03 Da, observed 957.05 Da.

MAPs were prepared for immunizations using a modified chemical ligation protocol.[45] Ligation was achieved by mixing the lysine core and peptide in 500 μL of solvent at certain pH value. The reaction was monitored by an analytical RP C8 column (Kromasil C8, The Nest Group, Inc., Southborough, MA, USA)

DOI: 10.1021/acsinfecdis.6b00006
ACS Infect. Dis. 2016, 2, 361–376

under UV214 nm wavelength. After it appeared complete, the reaction was quenched by adding 0.05% TFA to adjust the pH to 7.0. The final product was then purified by semipreparative HPLC at a flow rate of 4 mL/min. The ligated peptide was lyophilized and characterized by an Agilent LC-MSD TOF. The preparative conditions of MAPs are listed in Table S10.

Detailed conditions of each MAPs peptide are summarized: MAP-$S_{471-597}$ (0.3 mg of BrK_2KA reacted with 5.0 mg of $S_{471-503}$ peptide), MeCN/H_2O/DMSO (40:50:10 v/v/v) as mixture solvent, Na_2CO_3 adjusting pH 8.0, sonication assisting reaction, 30% yield, HPLC preparation by a gradient of 0−25% MeCN against water for 5 min, 25−40% MeCN for 50 min; MAP-$S_{604-625}$ (0.4 mg BrK_2KA reacted with 5.1 mg of $S_{604-625}$ peptide), MeCN/H_2O (25:75, v/v), Na_2CO_3 adjusting pH 7.8, 40% yield, HPLC preparation by a gradient of 0−25% MeCN against water for 5 min, 25−40% MeCN for 50 min; MAP-$S_{597-625}$ (0.35 mg of BrK_2KA reacted with 5.0 mg of $S_{597-625}$ peptide), MeCN/H_2O (50:50, v/v), Na_2CO_3 adjusting pH 8.5, 50% yield, HPLC preparation by a gradient of 0−25% MeCN against water for 5 min, 25−40% MeCN for 50 min; MAP-$S_{1164-1191}$(0.35 mg of BrK_2KA reacted with 5.0 mg of $S_{1164-1191}$ peptide), MeCN/H_2O (50:50, v/v), Na_2CO_3 adjusting pH 8.5, 42% yield, HPLC preparation by a gradient of 0−35% MeCN against water for 5 min, 35−40% MeCN for 50 min. Water and MeCN containing 0.1% TFA used for HPLC preparation were preprepared. The column and flow rate were a Vydac 208TP510 and 4 mL/min, respectively.

PEPscan (Peptide Screening) for Linear B-Cell Epitopes of SARS-CoV Recognized by Human Sera from SARS-CoV Recovered Patients. The studies of human sera to evaluate their levels of anti-SARS-CoV IgG that recognized the peptides were approved with an Expedited Review of Research Plan by the Institutional Review Board of Peking Union Medical College Hospital, Chinese Academy Medical Sciences & Peking Union Medical College (CAMS & PUMC). More than 500 antisera of SARS patients and 27 sera of healthy volunteers were involved in this study, which was conducted according to the guidelines for treatment of human subjects of the National Institutes of Health, USA. Written informed consent was obtained from all study participants.

The PEPscan was carried out as described by Hu et al.[35] without major modification. The optical density was read at 450 and 630 nm in an optical density reader (Labsystem, Franklin, MA, USA). The cutoff value was determined as twice the average value of the negative controls.

Binding of Mouse Monoclonal Antibodies to the SARS-CoV Virion. The SARS-CoV PUMC01 strain[46] was diluted with coating buffer to 4×10^{-5} $TCID_{50}$/mL (bicarbonate/carbonate coating buffer, 0.05 M, pH 9.6). The virus was then coated on 96-well plates with 100 μL (4×10^{-4} of $TCID_{50}$) of virus per well for 12 h at 4 °C. The coating buffer was removed from the wells, and 100 μL of blocking buffer was added per well and incubated for 12 h at 4 °C (2% BSA in PBS, pH 7.4; GIBCO, Carlsbad, CA, USA). The plates were washed twice with PBS (pH 7.2). The mouse monoclonal antibodies against SARS-CoV and control mAb against HIV-P27 were diluted to 0.001 μg/μL in the blocking buffer, added to the wells separately, and incubated for 1 h at 37 °C. The plates were washed twice with PBS and the secondary antibody (HRP-conjugated goat anti-mouse IgG, (GeneTex, Irvine, CA, USA) diluted 1:1000 in blocking buffer) was added to each well and incubated for 1 h at 37 °C. The secondary antibody was removed, the plate was washed three times with PBS, and then 100 μL of TMB substrate solution (Promega, Madison, WI, USA) was added to each well. After incubation for 30 min at room temperature, the absorbance of the test wells was read at 450 nm (A_{450}).

Analysis of Neutralization Using a Neutral Red Staining (NRS)-Based Assay. MAbs were serially diluted in DMEM culture medium. Human polyclonal antisera from convalescent SARS patients were diluted to 1:500 (v/v). The SARS-CoV PUMC01 strain was diluted with DMEM to 4×10^{-4} $TCID_{50}$. The NRS neutralization assay was performed in 96-well flat-bottom plates. The setup is similar to that of the cytopathic effect (CPE)-based neutralization assay. After incubation of 50 μL (4×10^{-4} $TCID_{50}$) of virus with 50 μL of antibodies or antisera in a total of 100 μL of DMEM medium per well for 1 h at 37 °C, Vero E6 cells (2×10^5 cells in 100 μL, from Cell Culture Center of PUMC) were added to each well. On day 5 of infection, when >70% of the cells showed CPE in the viral control wells (with DMEM instead of antibody or antisera), the culture medium was removed from the test wells and 100 μL of 0.15% neutral red (Sigma, St. Louis, MO, USA) in DMEM was added to each well. After incubation for 1 h at 37 °C, the neutral red medium was removed, the plates were washed twice with PBS (pH 7.2), and then 100 μL of acidified alcohol (1% acetic acid in 50% ethanol) was added to each well. After incubation for 30 min at room temperature, the absorbance of neutral red stained plates was read at 450 nm (A_{450}).

Percent neutralization was determined by the following formula: % neutralization = (A_{450} of antibody test wells − A_{450} of viral control wells)/(A_{450} of cell control wells − A_{450} of viral control wells) × 100.

Generation, Purification, and Measurement of the Affinity of Antipeptide Monoclonal Antibodies. Ganp-transgenic mice were originally established in a C57BL/6 strain as described previously.[47] The mice were backcrossed with BALB/c mice for at least eight generations and used for immunization to establish mAbs. All mice were maintained in specific pathogen-free conditions by the Center for Animal Resources and Development (CARD), Kumamoto University.

As immunogens, four peptides of $S_{471-503}$, $S_{604-625}$, $S_{597-625}$, and $S_{1164-1191}$ were synthesized and conjugated with keyhole limpet hemocyanin (KLH) by Operon Biotechnologies (Tokyo, Japan). One hundred micrograms of peptide−KLH emulsified in complete Freund's adjuvant (CFA) was injected subcutaneously as a primary immunization and boosted after 2 weeks with incomplete Freund's adjuvant (IFA). Sera of immunized mice were measured by ELISA using plates coated with free peptides. The mice with highest serum Ab titers were further immunized, and 4 days later the spleen cells were obtained for polyethylene glycol-mediated cell fusion with mouse myeloma cell line X63 using standard procedures.[48] The fused cells were selected with HAT medium in microculture plates at a concentration of 2×10^4 cells/well in the presence of IL-6 (5 units/mL).

The mAbs binding to the immunizing peptide Ags were detected with HRP-conjugated goat anti-mouse IgG Ab (Zymed, South San Francisco, CA, USA) with the substrate OPD (Wako Chemicals, Osaka, Japan). The positive signals (A_{490} > 1.0) were selected, and hybridomas were cloned by a limiting dilution method, adapted to serum-free media, and purified by protein G-Sepharose affinity chromatography (GE Healthcare, Buckinghamshire, UK). The purity of the antibodies was examined by SDS-PAGE and protein staining with Coomassie Brilliant Blue. The heavy and light chain isotypes were determined using an isotyping kit (BD Biosciences, Franklin Lakes, NJ, USA).

DOI: 10.1021/acsinfecdis.6b00006
ACS Infect. Dis. 2016, 2, 361−376

The affinity of the mAbs for peptides was determined by the BIAcore assay.[49] The on- and off-rate constants (k_{on} and k_{off}) for binding of the mAbs to $S_{471-503}$, $S_{604-625}$, $S_{597-625}$, and $S_{1164-1191}$ peptides (Table 1) were determined using the BIAcore system (BIAcore International AB, Uppsala, Sweden). The carboxylmethylated dextran surface of the sensor chip was activated with *N*-ethyl-*N*′-(3-dietylaminopropyl)carbodiimide and *N*-hydroxysuccinimide (EDC−EHS).[50] Each peptide was immobilized through the free thiol group of a cysteine residue that was deliberately placed at the N-terminus, by injection of 35 μL of a 20 μg/mL solution in 10 mM 2-(*N*-morpholino)ethanesulfonic acid buffer (pH 6) to the EDC−NHS-activated surface that had been reacted with 2-(2-pyridinyldithio)ethaneamine. The excess disulfide groups were deactivated by the addition of cysteine. The mAbs were diluted in 10 mM Hepes (pH 7.4), 150 mM NaCl, 3.4 mM EDTA, and 0.05% (v/v) BIAcore surfactant P20 and injected over the immobilized antigen at a flow rate of 5 μL/min. The association was monitored by the increase in the refractive index of the sensor chip surface per unit time. The dissociation of the mAbs was monitored after the end of the association phase with a flow rate of 50 μL/min. Kinetic rate constants were calculated from the collected data using the Pharmacia Kinetics Evaluation software.[51] The k_{on} was determined by measuring the rate of binding to the antigen at different protein concentrations.

Macaque Experiments. *Animals.* Rhesus monkeys (3−4 years old, Tables S4 and S6, from the Institute of Laboratory Animal Science) were examined according to the national microbiologic and parasite SPF standard and were determined free of anti-SARS antibody. The SPF monkeys were housed in an AAALAC-accredited facility before infection with SARS-CoV. The monkeys were then housed in a biosafety level 3 (BSL-3) facility for infection experiments. All procedures were approved by the Animal Use and Care Committee of the Institute of Laboratory Animal Science, Peking Union Medical College (Animal Welfare Assurance No. A5655-01, IACUC approval date September 24, 2007).

Challenges with SARS-CoV. Monkey challenges were performed in a BSL-3 facility.[37] Briefly, the animals were anesthetized with ketamine (0.5 mL/kg, im). The $TCID_{50}$ 10^{-6} (4.0 mL/monkey) of the stock PUMC01 strain virus was sprayed into the nasal cavity of the animals.

Pathologic Examination. The lung tissues were sampled from the euthanized animals. Organs were examined grossly, and photographs were taken to record the lung damage.

Samples of 5−10 g of lung tissues were collected from each lung and frozen at −80 °C. The remaining tissues were fixed in 10% formaldehyde for 1 week in the BSL-3 laboratory. The tissues were then processed in the regular pathology laboratory by dehydration, embedding, and sectioning.

For hematoxylin and eosin (H&E) staining, the sections were sequentially treated with xylene I, 10 min; xylene II, 10 min; 100% alcohol, 5 min; 95% alcohol, 5 min; 90% alcohol, 5 min; 80% alcohol, 5 min; 70% alcohol, 5 min; and PBS, 5 min. The sections were then stained in hematoxylin for 5 min; washed with tap water and double-distilled water for 5 s, with PBS for 5 min, with 95% alcohol for 30 s, with eosin for 30 s, with 95% alcohol for 5 s, with 100% alcohol I for 5 s, with 100% alcohol II for 5 s, with xylene I for 5 min, with xylene II for 5 min, and with xylene III for 5 min; and mounted with mounting buffer (ZhongShan Inc., Guangzhou, China).

Immunohistochemical Analysis of the Infected Lung Tissues. A mixture of the mouse monoclonal antibodies mAb-4E5 (0.01 μg/mL), mAb-11B1 (0.01 μg/mL), and mAb-9A6 (0.01 μg/mL) was used as primary antibody for the immunohistochemical analysis of the infected lung tissues. Briefly, tissue sections were treated with the primary antibody at 4 °C overnight, washed three times with PBS, incubated with HRP−goat-anti-mouse IgG (1:1000, ZhongShan Inc., PRC) at 37 °C for 30 min, and then washed three times with PBS. The DAB substrate (1:50) was added and incubated at 37 °C for 30 min and then stained with hematoxylin for 3 min.

RT-PCR for Analysis of the SARS-CoV Burden. The tissues from cranial and caudal lobes of the left lung and cranial, middle, and caudal lobes of the right lung from each animal were sampled and pooled together, and the total RNA was isolated from the lung tissues using Trizol (Invitrogen, USA). One hundred milligrams of lung tissue was mixed with 1 mL of Trizol extraction buffer and homogenized for 60 s (Homogenizer, IKA, Germany). The RNA wan then extracted with chloroform and precipitated with isopropanol. RNA was dissolved in 50 μL of DEPC water, and the RNA quality was verified by electrophoresis on agarose gel.

For the reverse transcription, 5 μg of total RNA was reverse transcribed with a high-capacity cDNA kit (RecertAid First Strand cDNA Synthesis Kit (Fermentas, Glen Burnie, MD, USA) with random hexamer primers. The reaction was performed at 42 °C for 60 min and terminated at 70 °C for 10 min.

Two microliters of reverse transcription mixture was used as template. The primers for SARS-CoV were 5′-ATGAATTAC-CAAGTCAATGGTTAC-3′ and 5′-CATAACCAGTCGGTA-CAGCTAC-3′. The PCR was normalized against monkey glyceraldehyde phosphate dehydrogenase (GAPDH) (NM002046). The GAPDH primers were 5′-TCAACAGCG-ACACCCACTC-3′ and 5′-CTTCCTCTTGTGCTCTTG-CTG-3′ (product size = 201 bp). The PCR was performed with a PCR kit (*Taq* DNA polymerase, Fermentas). The PCR products were detected by 1.6% agarose gel electrophoresis.

Reaction conditions were as follows: 10× *Taq* buffer (2 μL), 2 mM dNTP (2 μL), forward primer (20 μM, 0.4 μL), reverse primer (20 μM, 0.4 μL), *Taq* DNA polymerase (0.8 μL), 25 mM $MgCl_2$ (2 μL), template DNA (cDNA, 2 μL), H_2O (9.4 μL); step 1, 94 °C for 3 min; step 2, 94 °C for 30 s, 55 °C for 30 s, 72 °C for 30 s, for 26 cycles, then 72 °C for 10 min.

qRT-PCR for Analysis of the SARS-CoV Burden. The SARS-CoV fragment was prepared by RT-PCR. A 240 bp fragment of SARS-CoV was amplified and separated by 1.6% agarose electrophoresis. The DNA fragment was recovered from the gel with a gel extraction kit (MinElute Gel Extraction Kit, QIAGEN Stanford, Valencia, CA, USA). The recovered DNA was measured and adjusted to concentrations of 1×10^6, 1×10^5, 1×10^4, 1×10^3, 1×10^2, and 1×10^1 copies/μL, which were used to generate a standard curve. This known copy number standard curve was used to calculate the copy number of SARS-CoV mRNA in the infected lung tissues.

RT-PCR for the infected samples was performed under the same conditions used for standard curves with the Roche Light Cycler following the instructions for the SYBR Green Realtime PCR Master Mix (Toyobo, Osaka, Japan).

The copy number of the virus was detected as follows. Briefly, 2 μL of the reverse transcription mixture from step 1 was used as template. The primers for SARS-CoV were 5′-ATGAATTAC-CAAGTCAATGGTTAC-3′ and 5′-CATAACCAGTCGGTA-CAGCTAC-3′. The reaction was continued for 40 cycles under the conditions: 2 × QuantiTect SYBR Green PCR (10 μL), gorward primer (10 μM, 1 μL), teverse primer (10 μM, 1 μL), RNase-free water (3 μL), yemplate DNA (cDNA, 5 μL), total

DOI: 10.1021/acsinfecdis.6b00006
ACS Infect. Dis. 2016, 2, 361−376

volume (20 μL); step 1, 94 °C for 3 min; step 2, 94 °C for 15 s, 55 °C for 30 s, 72 °C for 20 s, for 40 cycles and then move to the melt curve procedure.

Immunization of Monkeys. The peptide and/or peptide mixtures were dissolved as 480 μg/mL of each peptide in 0.9% NaCl and then formulated with an equal volume of Freund's Complete Adjuvant (FCA) (Sigma, St. Louis, MO, USA) according to the manufacturer's instructions. The injected dose of vaccine was 0.5 mL/4 kg/monkey (120 μg/4 kg/monkey) given through intramuscular (im) injections at four sites on the arms and legs.

Rhesus monkeys were boosted at 2, 4, and 6 weeks after the first injection with the same dose of peptides and volume of vaccine as for the first injection, but formulated in an equal volume of Freund's incomplete adjuvant (IFA) (Sigma).

Venous blood samples (2 mL/each) were collected every 7 days from each monkey. The sera were isolated by centrifugation at 2000 rpm and immediately stored at −80 °C.

Antipeptidic IgG was detected by ELISA. Free peptides were diluted in carbonate buffer (pH 9.6) to a final concentration of 10 μg/mL. One hundred microliters of the peptide solution was added to 96-well polystyrene high BIND microplates (Corning Life Science, Santa Clara, CA, USA) for coating overnight at 4 °C. The wells of plates were then washed three times with PBS-Tween buffer (10 mM phosphate buffer, 150 mM NaCl, 0.05% Tween 20, pH 7.2) and subsequently blocked with 3% BSA in PBS-Tween buffer for an additional 1 h at 37 °C. After three thorough washings of the wells with PBS-Tween buffer, the antigen-coated microplates were incubated with diluted monkey sera at room temperature for 1 h. After three washings with PBS-Tween buffer, bound antibodies were detected with HRP-conjugated goat anti-monkey IgG (1:2000 v/v, Gene Tex). After three washings with PBS-Tween, a TMB substrate solution (Promega, Madison, WI, USA) was added and the color developed for 20 min before the reaction was stopped with 100 μL of 0.2 M H_2SO_4. The absorbance at 450 nm was read using a microtiter plate reader.

Macaques Treated by MAb43-3-14. Eighteen rhesus monkeys in six groups (Table S6, 3−4 years old) were examined according to the national microbiologic and parasite SPF standard and were verified free of anti-SARS antibody. mAb43-3-14 was adjusted to concentrations of 0.4 and 3.6 mg/mL with 0.9% NaCl, respectively. A dose of 0.2 or 1.8 mg/kg of the antibody given by intravenous (iv) injection was used to treat the different groups. The same volume of 0.9% NaCl was used for the control group. The procedures were approved by the Animal Use and Care Committee of the Institute of Laboratory Animal Science, Peking Union Medical College (Animal Welfare Assurance No. A5655-01, IACUC approval date September 24, 2007).

Statistical Analysis. All data were analyzed using Prism software (GraphPad software). For neutralization assays and ELISA, mean and standard deviation were used to determine significance. For qRT-PCR, geometric mean and standard deviation were used to determine virus burden.

■ ASSOCIATED CONTENT

Supporting Information

The Supporting Information is available free of charge on the ACS Publications website at DOI: 10.1021/acsinfecdis.6b00006.

Neutralization and enhancement of SARS-CoV infection of Vero E6 cells in the presence of human antisera of convalescent SARS patients, design and synthesis of new peptides, generated antipeptide mAbs, monkeys for peptide vaccine immunization against SARS-CoV, pathologic classification of the severity of the lung damage in SARS-CoV-infected rhesus macaques, conditions for preparation of multiple antigen peptides (PDF)

■ AUTHOR INFORMATION

Corresponding Authors

*(N.S.) E-mail: nobusaka@ifrec.osaka-u.ac.jp.
*(C.Q.) E-mail: qinchuan@pumc.edu.cn.
*(G.L.) E-mail: gangliu27@tsinghua.edu.cn.

Author Contributions

‖W.Q.D., Z.L.F., and K.K. equally contributed to this work.

Notes

The authors declare no competing financial interest.

■ ACKNOWLEDGMENTS

We are grateful to Professor Carl F. Nathan and Dr. Michael S. Diamond for their kind discussion and manuscript preparation. We thank Dr. Baoxing Fan for his serological evaluation of the large number of SARS-CoV convalescent antisera. The project described in this paper was supported by the National Institute of Allergy and Infectious Diseases (U01AI061092). The study was also partially supported for preparation of the monoclonal antibodies by contract research for MEXT for Emerging and Reemerging Infectious Diseases and Promotion of Fundamental Studies in Health Sciences (04-2) of the NIBIO and National Natural Science Foundation of China (No. 90713045). The funders had no role in study design, data collection and analysis, decision to publish, or preparation of the manuscript.

■ REFERENCES

(1) Hilgenfeld, R., and Peiris, M. (2013) From SARS to MERS: 10 years of research on highly pathogenic human coronavirus. *Antiviral Res. 100* (1), 286−295.

(2) Drosten, C., Günther, S., Preiser, W., van der Werf, S., Brodt, H. R., et al. (2003) Identification of a novel coronavirus in patients with severe acute respiratory syndrome. *N. Engl. J. Med. 348*, 1967−1976.

(3) Li, W., Shi, Z., Yu, M., Ren, W., Smith, C., et al. (2005) Bats are natural reservoirs of SARS-like coronaviruses. *Science 310*, 676−679.

(4) Guan, Y., Zheng, B. J., He, Y. Q., Liu, X. L., Zhuang, Z. X., Cheung, C. L., et al. (2003) Isolation and characterization of viruses related to the SARS coronavirus from animals in southern China. *Science 302*, 276−278.

(5) Marra, M. A., Jones, S. J., Astell, C. R., Holt, R. A., Brooks-Wilson, A., et al. (2003) The genome sequence of the SARS-associated coronavirus. *Science 300*, 1399−1404.

(6) Rota, P. A., Oberste, M. S., Monroe, S. S., Nix, W. A., Campagnoli, R., et al. (2003) Characterization of a novel coronavirus associated with severe acute respiratory syndrome. *Science 300*, 1394−1399.

(7) The Chinese SARS molecular epidemiology consortium . Molecular evolution of the SARS coronavirus during the course of the SARS epidemic in China. *Science* 2004, *303*, 1666−1669.10.1126/science.1092002

(8) Li, W., Moore, M. J., Vasilieva, N., Sui, J., Wong, S. K., et al. (2003) Angiotensin-converting enzyme 2 is a functional receptor for the SARS coronavirus. *Nature 426*, 450−454.

(9) Jeffers, S. A., Tusell, S. M., Gillim-Ross, L., Hemmila, E. M., Achenbach, J. E., et al. (2004) CD209L (L-SIGN) is a receptor for severe acute respiratory syndrome coronavirus. *Proc. Natl. Acad. Sci. U.S.A. 101*, 15748−15753.

(10) Wang, B., Chen, H., Jiang, X., Zhang, M., Wan, T., et al. (2004) Identification of an HLA-A*0201-restricted CD8+ T-cell epitope SSp-1 of SARS-CoV spike protein. *Blood 104*, 200−206.

DOI: 10.1021/acsinfecdis.6b00006
ACS Infect. Dis. 2016, 2, 361−376

(11) Wang, Y. D., Sin, W. Y., Xu, G. B., Yang, H. H., Wong, T. Y., et al. (2004) T-cell epitopes in severe acute respiratory syndrome (SARS) coronavirus spike protein elicit a specific T-cell immune response in patients who recover from SARS. *J. Virol. 78*, 5612−5618.
(12) Roberts, A., Wood, J., Subbarao, K., Ferguson, M., Wood, D., et al. (2006) Animal models and antibody assays for evaluating candidate SARS vaccines: summary of a technical meeting 25−26 August 2005, London, UK. *Vaccine 24*, 7056−7065.
(13) Gillim-Ross, L., and Subbarao, K. (2006) Emerging respiratory viruses: challenges and vaccine strategies. *Clin. Microbiol. Rev. 19*, 614−636.
(14) Graham, R. L., Donaldson, E. F., and Baric, R. S. (2013) A decade after SARS: strategies for controlling emerging coronaviruses. *Nat. Rev. Microbiol. 11* (12), 836−848.
(15) Yang, Z. Y., Werner, H. C., Kong, W. P., Leung, K., Traggiai, E., et al. (2005) Evasion of antibody neutralization in emerging severe acute respiratory syndrome coronaviruses. *Proc. Natl. Acad. Sci. U.S.A. 102*, 797−801.
(16) Dandekar, A. A., and Perlman, S. (2005) Immunopathogenesis of coronavirus infections: implications for SARS. *Nat. Rev. Immunol. 5*, 917−927.
(17) Subbarao, K., and Roberts, A. (2006) Is there an ideal animal model for SARS? *Trends Microbiol. 14*, 299−303.
(18) Taylor, D. R. (2006) Obstacles and advances in SARS vaccine development. *Vaccine 24*, 863−871.
(19) Takada, A., and Kawaoka, Y. (2003) Antibody-dependent enhancement of viral infection: molecular mechanisms and in vivo implications. *Rev. Med. Virol. 13*, 387−398.
(20) Tirado, S. M. C., and Yoon, K. J. (2003) Antibody-dependent enhancement of virus infection and disease. *Viral Immunol. 16*, 69−86.
(21) Gorlani, A., and Forthal, D. N. (2013) Antibody-dependent enhancement and the risk of HIV infection. *Curr. HIV Res. 11* (5), 421−426.
(22) Sullivan, N., Sun, Y., Binley, J., Lee, J., Barbas, C. F., 3rd, Parren, P. W., Burton, D. R., and Sodroski, J. (1998) Determinants of human immunodeficiency virus type 1 envelope glycoprotein activation by soluble CD4 and monoclonal antibodies. *J. Virol. 72* (8), 6332−6338.
(23) Guillon, C., Schutten, M., Boers, P. H., Gruters, R. A., and Osterhaus, A. D. (2002) Antibody-mediated enhancement of human immunodeficiency virus type 1 infectivity is determined by the structure of gp120 and depends on modulation of the gp120-CCR5 interaction. *J. Virol. 76* (6), 2827−2834.
(24) Gorlani, A., and Forthal, D. N. (2013) Antibody-dependent enhancement and the risk of HIV infection. *Curr. HIV Res. 11* (5), 421−426.
(25) Halstead, S. B. (2007) Dengue. *Lancet 370*, 1644−1652.
(26) Goncalvez, A. P., Engle, R. E., St, Claire, M., Purcell, R. H., and Lai, C. J. (2007) Monoclonal antibody-mediated enhancement of dengue virus infection in vitro and in vivo and strategies for prevention. *Proc. Natl. Acad. Sci. U.S.A. 104*, 9422−9427.
(27) Pierson, T. C., Xu, Q., Nelson, S., Oliphant, T., Grant, E., et al. (2007) The stoichiometry of antibody-mediated neutralization and enhancement of West Nile virus infection. *Cell Host Microbe 1*, 135−145.
(28) Taylor, A., Foo, S. S., Bruzzone, R., Dinh, L. V., King, N. J., and Mahalingam, S. (2015) Fc receptors in antibody-dependent enhancement of viral infections. *Immunol Rev. 268* (1), 340−364.
(29) Pierson, T. C., Sánchez, M. D., Puffer, B. A., Ahmed, A. A., Geiss, B. J., Valentine, L. E., Altamura, L. A., Diamond, M. S., and Doms, R. W. (2006) A rapid and quantitative assay for measuring antibody-mediated neutralization of West Nile virus infection. *Virology 346* (1), 53−65.
(30) Mehlhop, E., Ansarah-Sobrinho, C., Johnson, S., Engle, M., Fremont, D. H., Pierson, T. C., and Diamond, M. S. (2007) Complement protein C1q inhibits antibody-dependent enhancement of flavivirus infection in an IgG subclass-specific manner. *Cell Host Microbe 2* (6), 417−426.
(31) Huang, K. J., Yang, Y. C., Lin, Y. S., Huang, J. H., Lin, H. S., Yeh, T. M., Chen, S. H., Liu, C. C., and Lei, H. Y. (2006) The dual-specific binding of dengue virus and target cells for the antibody-dependent enhancement of dengue virus infection. *J. Immunol. 176*, 2825−2832.
(32) He, Y. X., Zhou, Y., Siddiqui, P., Niu, J., and Jiang, S. B. (2005) Identification of immunodominant epitopes on the membrane protein of the severe acute respiratory syndrome-associated coronavirus. *J. Clin Microbiol. 43* (8), 3718−3726.
(33) He, Y. X., Zhou, Y., Wu, H., Kou, Z. H., Liu, S. W., and Jiang, S. B. (2004) Mapping of Antigenic Sites on the Nucleocapsid Protein of the Severe Acute Respiratory Syndrome Coronavirus. *J. Clin Microbiol. 42* (11), 5309−5314.
(34) Liang, Y. F., Wan, Y., Qiu, Li. W., Zhou, J., Ni, B., Guo, B., Zou, Q., Zou, L. Y., Zhou, W., Jia, Z. C., Che, X. Y., and Wu, Y. Z. (2005) Comprehensive Antibody Epitope Mapping of the Nucleocapsid Protein of Severe Acute Respiratory Syndrome (SARS) Coronavirus: Insight into the Humoral Immunity of SARS. *Clin. Chem. 51* (8), 1382−1396.
(35) Hu, H., Li, L., Kao, R. Y., Kou, B., Wang, Z., et al. (2005) Screening and identification of linear B-cell epitopes and entry-blocking peptide of severe acute respiratory syndrome (SARS)-associated coronavirus using synthetic overlapping peptide library. *J. Comb. Chem. 7*, 648−656.
(36) Tam, J. P. (1988) Synthetic peptide vaccine design: synthesis and properties of a high-density multiple antigenic peptide system. *Proc. Natl. Acad. Sci. U.S.A. 85*, 5409−5413.
(37) Qin, C., Wang, J., Wei, Q., She, M., Marasco, W. A., et al. (2005) An animal model of SARS produced by infection of Macaca mulatta with SARS coronavirus. *J. Pathol. 206*, 251−259.
(38) Wong, S. K., Li, W., Moore, M. J., Choe, H., and Farzan, M. (2003) A 193-amino acid fragment of the SARS coronavirus S protein efficiently binds angiotensin-converting enzyme 2. *J. Biol. Chem. 279*, 3197−3201.
(39) Li, W., Zhang, C., Sui, J., Kuhn, J. H., Moore, M. J., et al. (2005) Receptor and viral determinants of SARS-coronavirus adaptation to human ACE2. *EMBO J. 24*, 1634−1643.
(40) Xu, Y., Zhu, J., Liu, Y., Lou, Z., Yuan, F., et al. (2004) Characterization of the heptad repeat regions, HR1 and HR2, and design of a fusion core structure model of the spike protein from severe acute respiratory syndrome (SARS) coronavirus. *Biochemistry 43*, 14064−14071.
(41) Xu, Y., Lou, Z., Liu, Y., Pang, H., Tien, P., et al. (2004) Crystal structure of severe acute respiratory syndrome coronavirus spike protein fusion core. *J. Biol. Chem. 279*, 49414−49419.
(42) Wang, S. F., Tseng, S. P., Yen, C. H., Yang, J. Y., Tsao, C. H., Shen, C. W., Chen, K. H., Liu, F. T., Liu, W. T., Chen, Y. M., and Huang, J. C. (2014) Antibody-dependent SARS coronavirus infection is mediated by antibodies against spike proteins. *Biochem. Biophys. Res. Commun. 451* (2), 208−214.
(43) Yip, M. S., Leung, N. H., Cheung, C. Y., Li, P. H., Lee, H. H., Daëron, M., Peiris, J. S., Bruzzone, R., and Jaume, M. (2014) Antibody-dependent infection of human macrophages by severe acute respiratory syndrome coronavirus. *Virol. J. 11*, 82.
(44) Jaume, M., Yip, M. S., Cheung, C. Y., Leung, H. L., Li, P. H., Kien, F., Dutry, I., Callendret, B., Escriou, N., Altmeyer, R., Nal, B., Daëron, M., Bruzzone, R., and Peiris, J. S. (2011) Anti-Severe Acute Respiratory Syndrome Coronavirus Spike Antibodies Trigger Infection of Human Immune Cells via a pH- and Cysteine Protease-Independent FcγR Pathwa. *J. Virol. 85* (20), 10582−10597.
(45) Dawson, P. E., Muir, T. W., Clark-Lewis, I., and Kent, S. B. (1994) Synthesis of proteins by native chemical ligation. *Science 266*, 776−779.
(46) Ruan, Y. J., Wei, C. L., Ee, A. L., Vega, V. B., Thoreau, H., Su, S. T., Chia, J. M., Ng, P., Chiu, K. P., Lim, L., Zhang, T., Peng, C. K., Lin, E. O., Lee, N. M., Yee, S. L., Ng, L. F., Chee, R. E., Stanton, L. W., Long, P. M., and Liu, E. T. (2003) Comparative full-length genome sequence analysis of 14 SARS coronavirus isolates and common mutations associated with putative origins of infection. *Lancet 361* (9371), 1779−1785.
(47) Sakaguchi, N., Kimura, T., Matsushita, S., Fujimura, S., Shibata, J., et al. (2005) Generation of High-Affinity Antibody against T Cell-Dependent Antigen in the Ganp Gene-Transgenic Mouse. *J. Immunol. 174*, 4485−4494.

DOI: 10.1021/acsinfecdis.6b00006
ACS Infect. Dis. 2016, 2, 361−376

(48) Kuwahara, K., Yoshida, M., Kondo, E., Sakata, A., Watanabe, Y., et al. (2000) A novel nuclear phosphoprotein, GANP, is up-regulated in centrocytes of the germinal center and associated with MCM3, a protein essential for DNA replication. *Blood 95*, 2321−2328.
(49) Jönsson, U. (1991) Real-time biospecific interaction analysis using surface plasmon resonance and sensor chip technology. *BioTechniques 11*, 620−627.
(50) Johnsson, B., Löfas, S., and Lindquist, G. (1991) Immobilization of proteins to a carboxymethyldextran-modified gold surface for biospecific interaction analysis in surface plasmon resonance sensors. *Anal. Biochem. 198*, 268−277.
(51) Karlsson, R., Michaelsson, A., and Mattsson, L. (1991) Kinetic analysis of monoclonal antibody-antigen interactions with a new biosensor based analytical system. *J. Immunol. Methods 145*, 229−240.

DOI: 10.1021/acsinfecdis.6b00006
ACS Infect. Dis. 2016, 2, 361−376